



1 **Photosynthesis-irradiance parameters of marine** 2 **phytoplankton: synthesis of a global data set**

3 Heather A. Bouman¹, Trevor Platt², Martina Doblin³, Francisco G. Figueiras⁴, Kristinn
4 Gudmundsson⁵, Hafsteinn G. Gudfinnsson⁵, Bangqin Huang⁶, Anna Hickman⁷, Michael
5 Hiscock⁸, Thomas Jackson², Vivian A. Lutz⁹, Frédéric Mélin¹⁰, Francisco Rey¹¹, Pierre Pepin
6 ¹², Valeria Segura⁹, Gavin H. Tilstone², Virginie van Dongen-Vogels³, Shubha
7 Sathyendranath²

8 ¹Department of Earth Sciences, University of Oxford, Oxford, OX1 3AN, United Kingdom

9 ²Plymouth Marine Laboratory, Prospect Place, The Hoe, PL1 3DH, United Kingdom

10 ³Plant Functional Biology and Climate Change Cluster, Faculty of Science, University of Technology Sydney, PO
11 Box 123 Broadway, Sydney, NSW 2007, Australia

12 ⁴Instituto de Investigaciones Marinas (CSIC), Eduardo Cabello 6, 36208 Vigo, Spain

13 ⁵Marine Research Institute, PO Box 1390, 121 Reykjavik, Iceland

14 ⁶State Key Laboratory of Marine Environmental Science/Key Laboratory of Coastal and Wetland Ecosystems,
15 Ministry of Education, Xiamen University, Xiamen, Fujian 361005, China

16 ⁷Ocean and Earth Science, University of Southampton, National Oceanography Centre Southampton, European
17 Way, Southampton, SO14 3ZH, United Kingdom

18 ⁸United States Environmental Protection Agency, Ariel Rios Building, 1200 Pennsylvania Avenue, Washington
19 D.C., 20460, U.S.A.

20 ⁹Instituto Nacional de Investigacion y Desarrollo Pesquero, Mar del Plata, Argentina

21 ¹⁰Institute for Environment and Sustainability, Joint Research Centre, European Commission, Ispra 21027, Italy

22 ¹¹Institute of Marine Research, c/o Department of Biological Sciences, University of Oslo, POB 1066, N-0316,
23 Oslo, Norway

24 ¹²Fisheries and Oceans Canada, Northwest Atlantic Fisheries Centre, PO Box 5667, St John's, Newfoundland,
25 A1C 5X1, Canada

26
27 *Correspondence to:* Heather A. Bouman (Heather.Bouman@earth.ox.ac.uk)

28
29 **Abstract.** The photosynthetic performance of marine phytoplankton varies in response to a
30 variety of factors, environmental and taxonomic. One of the aims of the MARine primary
31 Production: model Parameters from Space (MAPPS) project of the European Space Agency is
32 to assemble a global database of photosynthesis-irradiance (*P-E*) parameters from a range of
33 oceanographic regimes as an aid to examining the basin-scale variability in the
34 photophysiological response of marine phytoplankton and to use this information to improve
35 the assignment of *P-E* parameters in the estimation of global marine primary production using
36 satellite data. The MAPPS *P-E* Database, which consists of over 5000 *P-E* experiments,
37 provides information on the spatio-temporal variability in the two *P-E* parameters (the
38 assimilation number, P_m^B , and the initial slope, α^B , where the superscripts *B* indicate
39 normalisation to concentration of chlorophyll) that are fundamental inputs for models (satellite-
40 based and otherwise) of marine primary production that use chlorophyll as the state variable.
41 Quality-control measures consisted of removing samples with abnormally-high parameter



1 values and flags were added to denote whether the spectral quality of the incubator lamp was
2 used to calculate a broad-band value of α^B . The MAPPS database provides a
3 photophysiological dataset that is unprecedented in number of observations and in spatial
4 coverage. The database would be useful to a variety of research communities, including marine
5 ecologists, biogeochemical modellers, remote-sensing scientists and algal physiologists. The
6 compiled data are available at doi:10.1594/PANGAEA.874087 (Bouman et al., 2017).

7 **1 Introduction**

8
9 Although global estimates of marine primary production tend to converge on a number around
10 40 – 50 GT per annum, the accuracy and precision on regional scales of the estimation
11 protocols remain relatively poor, partly as a result of an incomplete understanding of how the
12 photosynthetic performance of marine phytoplankton varies in the global ocean (Carr et al.
13 2006, Lee et al. 2015). Photosynthesis-irradiance (*P-E*) parameters derived from carbon uptake
14 experiments conducted over a controlled range of available-light levels provide a means of
15 comparing the photosynthetic characteristics of marine phytoplankton across different natural
16 populations and cultured isolates (Platt and Jassby 1976, Prézelin et al. 1989, MacIntyre et al.
17 2002). The *P-E* experiment exposes algal cells to a range of light intensities from near-zero to
18 those levels typically available at the sea surface (Lewis and Smith 1983, Babin et al. 1994).
19 The photosynthetic rates are then normalised to the concentration of chlorophyll-a (a useful and
20 practical index of phytoplankton biomass relevant for photosynthesis) found within the sample.
21 This normalisation serves two purposes: first, dividing by pigment biomass reduces the
22 variability of photosynthesis rates due to differences in biomass alone, facilitating the
23 comparison of photosynthetic performance across trophic gradients, and second, chlorophyll-
24 normalised photophysiological parameters may be applied in the estimation of primary
25 production over large scales by using satellite-derived maps of chlorophyll concentration
26 (Longhurst et al. 1995, Antoine and Morel 1996). A schematic diagram showing the biomass-
27 normalised data generated from these experiments plotted against the light intensity at which
28 each bottle was incubated is shown in Fig. 1 to illustrate how the ensemble of data, when fitted
29 to a suitable non-linear equation, forms a *P-E* curve. The curve may be represented by a variety
30 of mathematical forms (Jassby and Platt 1976, Platt et al. 1980). In cases where
31 photoinhibition is negligible, all equations suitable for describing the *P-E* curve can be



1 represented using just two parameters: the initial slope, α^B , which represents the photosynthetic
 2 efficiency under light levels close to zero, and the asymptote of the curve, P_m^B , which is the
 3 photosynthetic rate at light saturation (Jassby and Platt 1976, Platt et al. 1980, Sakshaug et al.
 4 1997).

6 **2 Data**

7
 8 Chlorophyll-a concentrations and photosynthesis-irradiance (P - E) parameters collected from
 9 four oceanic domains and 35 biogeochemical provinces (Longhurst 2007, Table 1) were
 10 compiled from individual investigators and online data repositories (Table 2). P - E data were
 11 obtained by ^{14}C and ^{13}C (Argentine Sea) uptake experiments, with incubation times varying
 12 from 1.5 to 4 hours. Chlorophyll concentrations used to normalise the carbon fixation rates
 13 were measured using either High Performance Liquid Chromatography or the standard
 14 fluorometric method (Mantoura et al. 1997). The environmental variables and photosynthetic
 15 parameters included the MAPPS database and their corresponding units are listed in Table 3.
 16 Further details on the experimental methodology for individual field campaigns are provided in
 17 the original publications (see Table 2).

18
 19 Table 2 includes information on which functional form was fitted to the P - E data for each of
 20 the datasets used in this study. In cases where photoinhibition was absent (photosynthetic rates
 21 stayed independent of irradiance in the light-saturated range), or where the fit was applied to
 22 data unaffected by photoinhibition, a two-parameter curve fit was used, of the form:

$$P^B(E) = P_m^B \tanh\left(\frac{\alpha^B E}{P_m^B}\right), \quad (1)$$

23
 24 where $P^B(E)$ is the chlorophyll-normalised photosynthetic rate ($\text{mg C (mg chl-a)}^{-1} \text{ h}^{-1}$) and E is
 25 the available light, which in this study is expressed in $\mu\text{mol quanta m}^{-2} \text{ s}^{-1}$. The light saturation
 26 parameter, E_k , is defined by the following relationship

$$E_k = \frac{P_m^B}{\alpha^B} \quad (2)$$

27
 28 and is illustrated in Figure 1 by the drawing a line from the intersection of the initial slope with
 29 the plateau of the curve onto the abscissa and has dimensions of irradiance.

30



In most cases, however, data were fit to the three-parameter function of Platt et al. (1980), which describes also the decrease in photosynthetic rate with irradiances much higher than saturating light levels, as follows:

$$P^B(E) = P_s^B \left(1 - \exp \left(-\frac{\alpha^B E}{P_s^B} \right) \right) \exp \left(-\frac{\beta^B E}{P_s^B} \right), \quad (3)$$

where β^B is the photoinhibition parameter describing the decrease in photosynthetic rate at high irradiance and P_s^B is the hypothetical maximum photosynthetic rate in the absence of photoinhibition. Hence when $\beta^B = 0$, $P_s^B = P_m^B$. When photoinhibition was present, values of P_m^B were derived using the following equation:

$$P_m^B = P_s^B \left(\frac{\alpha^B}{\alpha^B + \beta^B} \right) \left(\frac{\beta^B}{\alpha^B + \beta^B} \right)^{\frac{\beta}{\alpha}}. \quad (4)$$

Quality Control for the MAPPS PE database

3.1 Experimental conditions

The P - E experiments were performed in incubators that maintained samples under in situ temperature conditions using either temperature-controlled water baths or the ship's underway water supply. Samples where incubation temperatures differed from in situ temperatures by more than 2 °C were removed from the database. It is well known that the light spectrum has a significant effect on the magnitude of light-limited photosynthesis (α^B) and the derived light saturation parameter (E_k) (Kyewalyanga et al. 1997; Schofield et al. 1991). We have included in the database quality flags indicating whether a correction factor for the spectrum of the lamp was applied to obtain a readily-intercomparable broad-band (white light) value (e.g. Kyewalyanga et al. 1997, Xie et al. 2015). This broad-band α^B combined with information on the shape of the phytoplankton absorption spectrum has been shown to provide an accurate estimate of the photosynthetic action spectrum $\alpha^B(\lambda)$. The correction factor X can be used to convert the measured α^B from the incubation experiment using a given artificial light source to an estimate of α^B if the sample were subject to a spectrally-neutral light environment: it is the



1 ratio of the unweighted mean absorption coefficient of phytoplankton (\bar{a}_p) to the mean
2 absorption coefficient weighted by the shape of the emission spectrum of the lamp source (\bar{a}_L)

$$X = \frac{\bar{a}_p}{\bar{a}_T}, \quad (5)$$

3
4 where \bar{a}_p is determined by

$$\bar{a}_p = \frac{\int_{400}^{700} a_p(\lambda) d\lambda}{\int_{400}^{700} d\lambda}, \quad (6)$$

5
6 and \bar{a}_T is computed as

$$\bar{a}_T = \frac{\int_{400}^{700} a_p(\lambda) E_T(\lambda) d\lambda}{\int_{400}^{700} E_T(\lambda) d\lambda}. \quad (7)$$

8
9 The incubators in this study used a range of light sources, including tungsten halogen, halogen,
10 metal halide, and fluorescent lamps. Tungsten halogen lamps are the most commonly-used
11 light source in *P-E* experiments because they provide intensities sufficiently high to resemble
12 irradiances at the sea surface ($\sim 2000 \mu\text{mol quanta m}^{-2} \text{s}^{-1}$). One limitation of using tungsten
13 lamps is that they have a spectrum heavily weighted towards the red and infrared (see Fig. 2),
14 unless the light first passes through a filter that removes the red emission. Table 4 describes the
15 various lamps and filters used in the *P-E* incubators used in this study.

16 To estimate the impact of a tungsten halogen lamp compared with a white light source on the
17 magnitude of the α^B and consequently E_k , which is derived from estimates of α^B (Equation 2),
18 we used a dataset from the North Atlantic that spanned several decades. From 1994, *P-E* data
19 have been corrected for the spectrum of the lamp source following the method of Kyewalyanga
20 et al. (1997), whereas prior to 1994, no correction was made due to a lack of information on the
21 excitation spectrum of the lamp and the absorptive properties of the phytoplankton
22 communities. By comparing data from similar regions and seasons as lamp sources have
23 changed, we are able to assess how the light source may cause variability in the photosynthetic
24 parameter α^B . In the post-1994 dataset, with corresponding lamp and absorption spectra, the
25 correction factor X varied from 1.30 to 2.06 (mean=1.70 with a standard deviation of 0.15).
26 This variation in X (Fig. 3a) is sufficient to account for difference in magnitudes of α^B obtained
27 using incubators with different light sources across the North Atlantic cruise dataset (Fig. 3b).
28 Note that potential errors in the computation of primary production due to changes in α^B caused
29 by spectral differences in light sources will be most acute deeper in the water column, where



1 the influence of the magnitude of α^B on primary production is greatest (Ulloa et al. 1997,
2 Bouman et al. 2000a) and thus errors for integrated water-column primary production will be
3 modest since productivity rates are highest at the surface and decrease in an exponential
4 manner once $E(z) \ll E_k$ (Ulloa et al. 1997, Bouman et al. 2000a).

5 3.1.1 Theoretical maxima

6 The photophysiological constraints of marine phytoplankton are well known, and provide a
7 useful check on the quality of the carbon-uptake experiments. The theoretical maximum
8 quantum yield of carbon fixation (ϕ_m^T) is $0.125 \text{ mol C (mol quanta)}^{-1}$ (Platt and Jassby 1976,
9 Sakshaug et al. 1997). The realised maximum quantum yield of photosynthesis (ϕ_m) is
10 calculated by dividing α^B by $\overline{a^*}$, the chlorophyll-specific absorption coefficient of
11 phytoplankton averaged over the visible spectrum (Platt and Jassby 1976) and multiplying by a
12 factor of 0.0231, which converts milligrams to moles of C, μmols to moles of photons, and
13 hours to seconds. Values of ϕ_m were calculated using either simultaneous measurements of $\overline{a^*}$,
14 or estimates derived from a global relationship between chlorophyll concentrations and $\overline{a^*}$
15 (Bouman, unpublished data) and samples with ϕ_m well above the theoretical maximum (>0.15
16 $\text{mol C (mol quanta)}^{-1}$) were discarded from the database. We also set a lower limit for the light
17 saturation parameter P_m^B of $0.2 \text{ mg C (mg chl-a)}^{-1} \text{ h}^{-1}$ and the initial slope α^B of 0.002 mg C (mg
18 $\text{chl-a)}^{-1} \text{ h}^{-1}$ ($\mu\text{mol quanta m}^{-2} \text{ s}^{-1}$) $^{-1}$. Data from experiments on sea-ice algae with chl-a
19 concentrations exceeding $50 \text{ mg chl-a m}^{-3}$ were also removed. Using these criteria, 278
20 experiments were excluded from the global database.

21 4 Results

22 4.1 Spatio-temporal patterns of the MAPPS *P-E* database

23 In this study we adopt the Longhurst's (2007) geographical classification system of domains
24 and provinces to partition the global dataset according to the prevailing physical conditions that
25 shape the structure and function of phytoplankton communities over large (basin) scales. The
26 rationale behind using Longhurst's approach to estimate primary productivity is that physical
27 forcing dictates the supply of nutrients and the average irradiance within the surface mixed
28 layer and these factors directly impact the physiological capacity of algal cells. The four



1 domains (also referred to as Longhurst biomes) are found in each ocean basin and are subject to
2 distinct mechanisms of physical forcing: in the polar domain the density structure of the surface
3 layer is strongly influenced by sea ice melt; in the westerlies domain the mixed layer dynamics
4 are governed by a local balance of heat-driven stratification and wind-driven turbulent mixing
5 by winds; in the trades domain, the depth of the mixed layer is governed by geostrophic
6 responses to seasonal changes in the strength and location of the trade winds and in the coastal
7 domain, terrestrial influx of freshwater and interaction of local winds with topography play a
8 critical role in governing ecosystem properties. The next level of partition is biogeochemical
9 provinces, which embrace a wider set of environmental factors that govern regional ocean
10 circulation and stratification that in turn influence ecological structure. Although it would be
11 preferable that both domain and provincial boundaries were dynamic to accommodate seasonal,
12 annual and decadal changes in ocean circulation (Devred et al. 2007), to exploit the entire
13 MAPPS *P-E* parameter dataset, which contains a large number samples that were collected
14 prior to the launch of ocean-colour satellites, we used the fixed rectilinear boundaries of
15 Longhurst (2007) with the understanding that some of the within-province variability may be
16 the result of the estimated and actual provincial boundaries being spatially offset.

17

18 Roughly half of the quality-controlled samples were collected from within the upper 20 m of
19 the water column, accounting for approximately 54% of the dataset. Most of the data fall
20 within the Atlantic Basin (Fig. 4), with a large region of the Pacific Basin being grossly
21 undersampled in both space and time. The latitudinal coverage of the database is relatively
22 sparse in the tropics and the mid-latitudes of the Southern Hemisphere. The seasonal
23 distribution of data shows the majority of samples were collected during the spring (40%),
24 summer (34%) and fall (22%), and only 3% of the samples collected during the winter period
25 (Table 2, Fig. 5). Across all seasons, the dataset covers a range of trophic conditions, from
26 highly oligotrophic conditions (0.02 mg m^{-3}) to spring bloom conditions (39.8 mg m^{-3}) (Fig. 6).
27 The dynamic range of the photosynthetic parameters was similar to that reported in other global
28 studies, with values P_m^B ranging from 0.21 and $25.91 \text{ mg C (mg chl-a)}^{-1} \text{ h}^{-1}$ with an average
29 value of 3.11 and a standard deviation = 2.28 and values of α^B ranging from 0.002 to 0.373 mg
30 $\text{C (mg chl-a)}^{-1} \text{ h}^{-1} (\mu\text{mol quanta m}^{-2} \text{ s}^{-1})^{-1}$ with an average value of 0.043 and a standard
31 deviation of 0.034.

32



1 The P - E parameters exhibited both spatial (between provinces) and temporal (between seasons)
2 differences. In general, values of the assimilation number increased with decreasing latitude
3 (Table 2) and tended to be higher during the summer months in temperate marine systems.
4 However, the seasonal and latitudinal bias in data coverage has important implications for
5 variability in parameter values in the dataset because of the environmental conditions known to
6 influence phytoplankton photophysiology. High-latitude samples will be associated with lower
7 temperatures, which may limit their maximum photosynthetic rate for carbon fixation (Smith
8 Jr. and Donaldson et al. 2015), and this is reflected in the generally low values of P_m^B in the
9 Boreal (BPLR) and Austral (APLR) Polar provinces. Geographical variation in surface
10 irradiance may also explain the lower values of P_m^B in high latitudes compared with low
11 latitudes. The combination of lower surface irradiances and deep convective mixing in high
12 latitudes results in markedly lower light levels within the mixed-layer, which may result in
13 photoacclimation to lower light levels, by modulating pigment content per cell and hence the
14 carbon-to-chlorophyll ratio (Cullen et al. 1982, Sathyendranath et al. 2009). However, it is
15 important to note that some of the polar samples were collected in regions highly influenced by
16 sea-ice melt, which may lead to the formation of a fresh, shallow and highly-stable mixed layer,
17 and consequent higher average light level than would be the case for deeper mixing.
18
19 The paucity of winter data reduces the number of samples with cells acclimated to low growth
20 irradiances. The number of observations is also low within the tropical and sub-tropical oceans
21 which are characterised by warm and hence strongly-stratified mixed layers. Phytoplankton
22 cells in these regions tend to have higher upper bounds of P_m^B , due to the combined effect of
23 warmer sea-surface temperatures and the acclimation to high-light conditions. Such spatio-
24 temporal patterns in the P - E parameters are likely driven by changes in oceanographic
25 conditions (temperature, stratification, macro- and micronutrient availability) (Geider et al.
26 1996) as well as in community structure and other biotic processes that may consume cellular
27 energy at the expense of carbon fixation (Puxty et al., 2016).

28

29 4.2 Relationship between the maximum photosynthetic rate and the initial slope

30



Strong correlations have been reported between the two P - E parameters P_m^B and α^B , which have been explained on both ecological and photophysiological grounds (Platt and Jassby 1976, Côté and Platt, 1983, Behrenfeld et al. 2004). The MAPPS dataset shows that the data fall largely within the bounds of E_k values between 20 and 300 $\mu\text{mol quanta m}^{-2} \text{s}^{-1}$ (Fig. 7). In general, high-latitude samples ($> 65^\circ$) tend to have lower P_m^B values for a given value of α^B (E_k values averaging 57.7 $\mu\text{mol quanta m}^{-2} \text{s}^{-1}$ with 10.0% of the data falling above 100 $\mu\text{mol quanta m}^{-2} \text{s}^{-1}$) when compared with low latitude samples between 40°N and 40°S (E_k values averaging 152.4 $\mu\text{mol quanta m}^{-2} \text{s}^{-1}$, with 57.1% of the values falling above 100 $\mu\text{mol quanta m}^{-2} \text{s}^{-1}$).

When E_k is plotted as a function of latitude (Fig. 8) for open-ocean samples within the top 25m of the water column, a clear pattern emerges, with higher latitude samples being characterised by lower values, whereas data from the mid-to-low latitudes had, on average, higher values, although considerable scatter was observed over the entire range of temperatures. To illustrate the depth-dependent change in E_k due to vertical changes in irradiance, data from cruises that predominantly sampled stratified, oligotrophic regions (DCM and AMT cruises) are plotted against the sample depth. The strong depth-dependence of the photoacclimation parameter is consistent with other open-ocean studies (Babin et al. 1996). The latitudinal and depth dependence of E_k was also reported in a study which used a subset ($N=1862$) of the MAPPS database from the North Atlantic spanning the Tropics to the Arctic: 55% of the variance in E_k could be explained using depth, latitude, temperature, nitrate and surface noon irradiance as predictive variables (Platt and Sathyendranath 1995).

5 Discussion

Predicting the photosynthetic efficiency of phytoplankton cells remains one of the major challenges in determining marine primary production using remote sensing data (Carr et al. 2006). The MAPPS database of P - E parameters allows us to assess the global variability in phytoplankton photophysiological parameters and could be used to validate models that aim to provide a mechanistic understanding of changes in the photosynthetic parameters. Here, we attempt to explain the spatial patterns in the dataset drawing on our current understanding of the key environmental factors governing variability in both P_m^B and α^B .



1 A positive correlation between P_m^B and α^B has been attributed to a variety of physiological and
2 ecological factors, including changes in the allocation of ATP and NADPH to carbon fixation
3 (Behrenfeld et al., 2004), as well as changes in phytoplankton community structure (Côté and
4 Platt, 1983). To disentangle the ecological from the physiological sources of variability is not
5 straightforward, unless additional information on the taxonomic composition and
6 photoacclimatory status of natural phytoplankton samples is available. Moreover, culture
7 studies have invoked viral infection as another potential source of variability that is poorly
8 understood in natural marine systems (Puxty et al. 2016).

9
10 Both taxon-specific and size-specific differences in P_m^B and α^B have been reported in both
11 culture and field studies (Bouman et al. 2005, Côté and Platt 1983, 1984, Huot et al. 2013, Xie
12 et al. 2015). As new remote-sensing algorithms are now starting to yield information on the
13 size and taxonomic structure of phytoplankton, it would be useful to derive additional
14 information on the P - E response of key phytoplankton taxa and size classes, especially those
15 implicated as playing key roles in ocean biogeochemical cycles (LeQuéré et al. 2005, Nair et al.
16 2008, Bracher et al. 2017). Although detailed information on the taxonomic and size structure
17 of ship-based experiments was lacking for several of the samples included in this dataset, more
18 recent studies include some measure of phytoplankton community structure, whether it be from
19 use of pigment markers, size fraction of pigment and/or productivity, or cell counts. Although
20 there is a question as to what the standard indices of community structure should be that can
21 help account for community-based variation in the photophysiological parameters across
22 datasets, it is likely that information on gross community structure alone will not account for a
23 large fraction of the variability in P - E parameters, especially across regions or seasons with
24 different environmental forcing (Bouman et al. 2005, Smith Jr. and Donaldson 2015) or
25 resident ecotypes (Geider and Osborne 1991).

26
27 The high range of photosynthetic parameters recorded at lower latitudes is largely caused by
28 depth-dependent changes due to photoacclimation and photoadaptation (Babin et al. 1996,
29 Bouman et al. 2000b, Huot et al. 2007) in highly stratified waters. Strong vertical gradients in
30 nutrient supply and growth irradiance lead to a vertical layering of ecological niches resulting
31 in strong vertical gradients in species composition and in the case of marine picocyanobacteria,
32 high-light and low-light ecotypes, are observed (Johnson et al. 2006, Zwirgmaier et al. 2007).



1 Although depth-dependent variability in the photosynthetic parameters can be examined in the
2 MAPPS dataset, in particular E_k (Fig. 9), it has been argued that optical depth may be a more
3 useful predictor of changes in the $P-E$ parameters resulting from vertical changes in the
4 photoacclimatory status of phytoplankton cells (Babin et al. 1996, Bouman et al. 2000b). In
5 highly stratified and stable seas such as the oligotrophic gyres this may be the case, yet in more
6 dynamic ocean conditions such as the Beaufort Sea, optical depth has been shown to have no
7 more predictive skill, and sometimes less, than using depth alone (Huot et al. 2013). It is
8 important to note that diel changes in the $P-E$ parameters were not taken into account in this
9 meta-analyses due to a lack of information on the time of sample collection in a significant
10 number of observations, which can be a significant source of variability (MacCaull and Platt
11 1977, Prézelin and Sweeney 1977, Prézelin et al. 1986, Harding et al. 1983, Cullen et al. 1992,
12 Bruyant et al. 2005). However, as noted in the study of Babin and co-authors (1996) such diel
13 and day-to-day variability in the $P-E$ parameters is likely to be far smaller when compared with
14 differences across biogeochemical provinces subject to markedly different environmental
15 forcing.

16

17 Clear latitudinal differences in the range of E_k values are revealed in the MAPPS dataset (Fig.
18 8) which suggests that E_k may be controlled by environmental factors that vary strongly with
19 latitude, such as temperature and the availability of light. Figure 8 shows that samples collected
20 from high-latitude environments, such as the Laborador Sea, the (sub)Arctic and the Southern
21 Ocean have markedly lower E_k values, reflecting the physical constraints of low temperatures
22 and, in some cases, low light levels (Harrison and Platt 1985). The physical dynamics of the
23 upper ocean and their impact on temperature and light conditions have been shown to play a
24 dominant role in governing the photosynthetic performance of polar and temperate marine
25 phytoplankton (Harrison and Platt, 1986, Bouman et al, 2005).

26 **6 Recommendations for use**

27 The MAPPS database of photosynthesis-irradiance parameters may be used to compute marine
28 primary production using remotely-sensed data on ocean colour (e.g. Longhurst et al. 1995).
29 The data present in Table 2 provide seasonal values of the photosynthetic parameters for
30 Longhurst biogeochemical provinces, whose geographical boundaries can be found online at
31 <http://www.marineregions.org/>. This dataset will also serve as a useful resource for validation



1 of other methods used to extrapolate *P-E* parameters to basin scales using ocean observables
2 (Antoine and Morel 1996, Platt et al. 2008, Saux-Picart et al. 2014). The MAPPS database will
3 allow such extrapolation procedures to be further tested and refined over a much larger range of
4 geographical and biogeochemical domains or for new approaches of parameter assignment to
5 be developed.

6

7 **6 Data availability**

8 The compiled data set containing 5711 individual photosynthesis-irradiance experiments is
9 and corresponding metadata are available on PANGAEA (<https://doi.pangaea.de>): doi:
10 10.1594/PANGAEA.874087 (Bouman et al. 2017).

11 **Acknowledgements**

12

13 The authors wish to thank the research scientists, technicians, students and crew who
14 contributed to the collection of these data. In particular, we acknowledge the significant
15 contributions made by Brian Irwin, Jeff Anning, Gary Maillet, Christine Hanson, Brian
16 Griffiths, James McLaughlin, Richard Matear, and Andy Steven.

17 **References**

- 18 Antoine, D., and Morel, A.: Oceanic primary production 1. Adaptation of a spectral light-
19 photosynthesis model in view of application to satellite chlorophyll observations. Glob.
20 Biogeochem. Cycles 10, 43-55, 1996.
- 21 Babin, M., Morel, A., and Gagnon, R: An incubator designed for extensive and sensitive
22 measurements of phytoplankton photosynthetic parameters, Limnol. Oceanogr., 39,
23 694–702, 1994.
- 24 Babin, M., Morel, A., Claustre, H., Bricaud, A., Kolber, Z., and Falkowski, P. J.: Nitrogen- and
25 irradiance-dependent variations of maximum quantum yield of carbon fixation in
26 eutrophic, mesotrophic and oligotrophic marine systems. Deep-Sea Res., 43, 1241-
27 1272, 1996.



- 1 Behrenfeld, M. J., Prasil, O., Babin, M., and Bruyant, F.: In search of a physiological basis for
2 covariations in light-limited and light-saturated photosynthesis. J. Phycol. 40, 4-25,
3 2004.
- 4 Bouman, H.A., Platt, T., Kraay, G.W., Sathyendranath, S., and Irwin, B.D.: Bio-optical
5 properties of the subtropical North Atlantic. I. Vertical variability. Mar. Ecol. Progr.
6 Ser. 200, 3–18, 2000b.
- 7 Bouman, H.A., Platt, T., Sathyendranath, S., Irwin, B.D., Wernand, M.R., and Kraay, G.W.: Bio-
8 optical properties of the subtropical North Atlantic. II. Relevance to models of primary
9 production. Mar. Ecol. Progr. Ser. 200, 19-34, 2000a.
- 10 Bouman, H. A., Platt, T., Sathyendranath, S., and Stuart, V.: Dependence of light-saturated
11 photosynthesis on temperature and community structure. Deep-Sea Res., 52, 1284-
12 1299, 2005.
- 13 Bracher, A., Bouman, H.A., Brewin, R.J.W., Bricaud, A., Brotas, V., Ciotti, A.M., Clementson,
14 L., Devred, E., Di Cicco, A., Dutkiewicz, S., Hardman-Mountford, N.J., Hickman, A.E.,
15 Hieronymi, M., Hirata, T., Losa, S.N., Mouw, C.B., Organelli, E., Raitsos, D.E., Uitz,
16 J., Vogt, M., and Wolanin, A.: Obtaining Phytoplankton Diversity from Ocean Color: A
17 Scientific Roadmap for Future Development. Front. Mar. Sci. 4:55. doi:
18 10.3389/fmars.2017.00055, 2017.
- 19 Bruyant, F., Babin, M. Genty, B., Prasil, O., Behrenfeld, M.J., Claustre, H., Bricaud, A.,
20 Garczarek, L., Holtzendorff, J., Koblizek, M., Dousova, H., and Partensky, F.: Diel
21 variations in the photosynthetic parameters of *Prochlorococcus* strain PCC 9511:
22 combined effects of light and cell cycle. Limnol. Oceanogr. 50, 850-863, 2005.
- 23 Carr, M. E., Friedrichs, M., Schmeltz, M., NoguchiAita, M., Antoine, D., Arrigo, K. R.,
24 Asanuma, I., Aumont, O., Barber, R., Behrenfeld, M. J., Bidigare, R., Buitenhuis, E.,
25 Campbell, J. W., Ciotti, A., Dierssen, H. M., Dowell, M., Dunne, J., Esaias, W., Gentili,
26 B., Gregg, W. W., Groom, S. B., Hoepffner, N., Ishizaka, J., Kameda, T., Le Quere, C.,
27 Lohrenz, S., Marra, J., Melin, F., Moore, K., Morel, A., Reddy, T., Ryan, J., Scardi, M.,
28 Smyth, T., Turpie, K., Tilstone, G. H., Waters, K., and Yamanaka, Y.: A comparison of
29 global estimates of marine primary production from ocean color. Deep Sea Res. II
30 53,741–770, 2006.
- 31 Cullen, J. J.: The deep chlorophyll maximum: comparing vertical profiles of chlorophyll a. Can.
32 J. Fish. Aquat. Sci. 39, 791-803, 1982.



- 1 Cullen, J. J., Lewis, M. R., Davis, C. O., and Barber, R. T.: Photosynthetic characteristics and
2 estimated growth rates indicate grazing is the proximate control of primary production
3 in the equatorial Pacific. *J. Geophys. Res.* 97, 639-654, 1992.
- 4 Côté, B. and Platt, T.: Utility of the light-saturation curve as an operational model for
5 quantifying the effects of environmental conditions on phytoplankton photosynthesis.
6 *Mar. Ecol. Progr. Ser.* 18, 57–66, 1984.
- 7 Côté, B. and Platt, T.: Day-to-day variations in the spring-summer photosynthetic parameters of
8 coastal marine phytoplankton. *Limnol. Oceanogr.* 28, 320-344, 1983.
- 9 Devred E., Sathyendranath S. and Platt T.: Delineation of ecological provinces using ocean
10 colour radiometry, *Mar. Ecol. Progr. Ser.* 346:1-13, 2007.
- 11 Dogliotti, A. I., Lutz, V. A., and Segura, V.: Estimation of primary production in the southern
12 Argentine continental shelf and shelf-break regions using field and remote sensing data.
13 *Rem. Sens. Env.*, 140, 497-508, 2014.
- 14 Eppley, R.W.: Temperature and phytoplankton growth in the sea. *Fishery Bull.* 70, 1063–1085,
15 1972.
- 16 Geider, R. J., MacIntyre, H. L., and Kana, T. M.: A dynamic model of photoadaptation in
17 phytoplankton. *Limnol. Oceanogr.* 41, 1-15, 1996.
- 18 Geider, R.J. and Osborne, B.A.: *Algal photosynthesis: The measurement of gas exchange and*
19 *related processes.* Chapman and Hall, New York, 256 pp., 1991.
- 20 Griffiths, F. B., Bates, T. S., Quinn, P. K., Clementson, L. A. and Parslow, J. S.:
21 Oceanographical context of the first Aerosol Characterisation Experiment (ACE-1): A
22 physical, chemical and biological overview. *J. Geophys. Res.* 104, 21649-21671, 1999.
- 23 Gudmundsson, K.: Long-term variation in phytoplankton productivity during spring in Icelandic
24 waters. *ICES J. Mar. Sci.*, 55, 635-643, 1998.
- 25 Hanson, C. E., Pattiaratchi, C. B., Waite, A. M.: Sporadic upwelling on a downwelling coast:
26 Phytoplankton responses to spatially variable nutrient dynamics off the Gascoyne region
27 of Western Australia. *Cont. Shelf Res.*, 25, 1561-1582, 2005.
- 28 Hanson, C. E., Pattiaratchi, C. B., and Waite, A. M.: Seasonal production regimes off south-
29 western Australia: influence of the Capes and Leeuwin Currents on phytoplankton
30 dynamics. *Mar. Freshwater Res.*, 56, 1011-1026, 2005.



- 1 Harding, L. W., Meeson, B. W., and Tyler, M. A.: Photoadaptation and diel periodicity of
2 photosynthesis in the dinoflagellate *Prorocentrum mariaelebouriae*. Mar. Ecol. Progr.
3 Ser. 13, 73-85, 1983.
- 4 Harrison, W. G., and Platt, T.: Photosynthesis-irradiance relationships in polar and temperate
5 phytoplankton populations. Polar Biol 5, 153–164, 1986.
- 6 Hickman, A. E.: The photophysiology and primary productivity of phytoplankton within the
7 deep chlorophyll maximum. Doctoral Thesis, University of Southampton, Doctoral
8 Thesis, 237 pp., 2007.
- 9 Hiscock, M. R., Marra, J., Smith Jr., W. O., Goericke, R., Measures, C., Vink, S., Olson, R. J.,
10 Sosik, H. M., and Barber, R. T. Primary productivity and its regulation in the Pacific
11 Sector of the Southern Ocean. Deep-Sea Res. II, 50, 533-558, 2003.
- 12 Hiscock, M. R.: The regulation of primary productivity in the Southern Ocean. Doctoral Thesis,
13 Duke University, 120 pp., 2004.
- 14 Huot, Y., Babin, M., Bruyant, F., Grob, C., Twardowski, M. S., and Claustre, H.: Does
15 chlorophyll a provide the best index of phytoplankton biomass for primary productivity
16 studies? Biogeosci. Discuss. 4, 707-745, 2007.
- 17 Huot, Y., Babin, M., and Bruyant, F.: Photosynthetic parameters in the Beaufort Sea in relation
18 to the phytoplankton community structure. Biogeosci. 10, 3445–3454, 2013.
- 19 Jassby, A. D. and Platt T.: Mathematical formulation of the relationship between photosynthesis
20 and light for phytoplankton. Limnol. Oceanogr. 21, 540-547, 1976.
- 21 Johnson, Z. I., Zinser, E. R., Coe, A. , McNulty, N. P. , Woodward, E. M. S., and Chisholm, S.
22 W.: Niche partitioning among *Prochlorococcus* ecotypes along ocean-scale
23 environmental gradients. Science, 311, 1737-40, 2006.
- 24 Kyewalyanga, M. N., Platt, T., and Sathyendranath, S.: Estimation of the photosynthetic action
25 spectrum: implication for primary production models. Mar. Ecol. Progr. Ser., 146, 207-
26 223, 1997.
- 27 Kyewalyanga, M.N., Platt, T., Sathyendranath, S., Lutz, V. A., and Stuart, V.: Seasonal variation
28 in physiological parameters of phytoplankton across the North Atlantic. J. Plankton Res.
29 20, 17-42, 1998.
- 30 Lawrenz, E., Silsbe, G., Capuzzo, E., Ylöstalo, P., Forster, R. M., Simis, S. G. H., Prásil, O.,
31 Kromkamp, J. C., Hickman, A. E., Moore, C. M., Forget, M.-H., Geider, R. J. and



- 1 Suggett, D. J.: Predicting the electron requirement for carbon fixation in seas and oceans.
- 2 PLoS ONE 8(3): e58137. doi:10.1371/journal.pone.0058137, 2013.
- 3 Lee, Y. J. and 25 others: An assessment of phytoplankton primary productivity in the Arctic
- 4 Ocean from satellite ocean color/in situ chlorophyll-a based models. J. Geophys. Res.
- 5 120, 6508-6541, 2015.
- 6 Le Quéré, C., Harrison, S. P., Prentice, I. C., Buitenhuis, E. T., Aumont, O., Bopp, L., Claustre,
- 7 H., da Cunha, L. C., Geider, R., Giraud, X., Klaas, C., Kohfeld, K. E., Legendre, L.,
- 8 Manizza, M., Platt, T., Rivkin, R. B., Sathyendranath, S., Uitz, J., Watson, A. J., and
- 9 Wolf-Gladrow, D.: Ecosystem dynamics based on plankton functional types for global
- 10 ocean biogeochemistry models. Global Change Biol. 11, 2016-2040, 2005.
- 11 Lewis, M. R., and Smith, J. C.: A small volume, short-incubation time method for measurement
- 12 of photosynthesis as a function of incident irradiance. Mar. Ecol. Progr. Ser. 13, 99-102,
- 13 1983.
- 14 Longhurst, A., Sathyendranath, S., Platt, T., and Caverhill, C.: An estimate of global primary
- 15 production in the ocean from satellite radiometer data. J. Plankton Res. 17, 1245–1271,
- 16 1995.
- 17 Longhurst, A. R.: Ecological Geography of the Sea. Academic Press, London, 2007.
- 18 Lorenzo, L.M., Arbones, B., Figueiras, F. G., Tilstone, G. H., Figueroa, F. L.: Photosynthesis,
- 19 primary production and phytoplankton growth rates in Gerlache and Bransfield Straits
- 20 during Austral summer: cruise FRUELA 95. Deep-Sea Res. II 49, 707-721, 2002.
- 21 Lutz, V. A., Segura, V., Dogliotti, A. I., Gagliardini, D. A., Bianchi, A. A., and Balestrini, C. F.:
- 22 Primary production in the Argentine Sea during spring estimated by field and satellite
- 23 models. J. Plankton Res., 32, 181-195, 2010.
- 24 MacCaull, W. A., and Platt, T.: Diel variations in the photosynthetic parameters of coastal
- 25 marine phytoplankton. Limnol. Oceanogr. 22, 723-731, 1977.
- 26 MacIntyre, H. L., Kana, T. M., Anning, T., and Geider, R. J.: Photoacclimation of
- 27 photosynthesis irradiance response curves and photosynthetic pigments in microalgae and
- 28 cyanobacteria. J. Phycol., 38, 17-38, 2002.
- 29 Mackey, D. J., Parslow, J. S., Higgins, H. W., Griffiths, F. B., O'Sullivan, J. E.: Plankton
- 30 productivity and biomass in the western equatorial Pacific: Biological and physical
- 31 controls. Deep-Sea Res. II 42, 499-533, 1995.



- 1 Mantoura, R. F. C., Jeffrey, S. W., Llewellyn, C. A., Claustre, H., and Morales, C.
2 E.: Comparison between spectrophotometric, fluorometric and HPLC methods for
3 chlorophyll analysis. In: Jeffrey SW, Mantoura RFC, Wright SW (eds) Phytoplankton
4 pigments in oceanography: Guidelines to modern methods. UNESCO, Paris, p 361, 1997.
- 5 Nair, A., Sathyendranath, S., Platt, T., Morales, J., Stuart, V., Forget, M.-H., Devred, E.,
6 Bouman, H.: Remote sensing of phytoplankton functional types. Remote Sens. Environ.
7 112: 3366–3375, 2008.
- 8 Pálsson, Ó. K., Gislason, A., Guðfinnsson, H. G., Gunnarsson, B., Ólafsdóttir, S. R., Petursdóttir,
9 H., Sveinbjörnsson, S., Thorisson, K., and Valdimarsson, H. Ecosystem structure in the
10 Iceland Sea and recent changes to the capelin (*Mallotus villosus*) population. ICES J.
11 Mar. Sci. doi:10.1093/icesjms/fss071, 2012.
- 12 Platt, T., Gallegos, C. L., and Harrison, W. G.: Photoinhibition of photosynthesis in natural
13 assemblages of marine phytoplankton. J. Mar. Res. 38, 687-701, 1980.
- 14 Platt, T., Harrison, G., Irwin, B., and Horne, E. P.: Photosynthesis and photoadaptation in the
15 arctic. Deep Sea Res. 29, 1159-1170, 1982.
- 16 Platt, T., and Jassby, A. D.: The relationship between photosynthesis and light for natural
17 assemblages of coastal marine phytoplankton. J. Phycol. 12, 421-430, 1976.
- 18 Platt, T., and Sathyendranath, S.: Latitude as a factor in the calculation of primary production In:
19 Ecology of Fjords and Coastal Waters, eds. H.R. Skjoldal, C. Hopkins, K.E. Erikstad,
20 H.P. Leinaas. Elsevier Science, 1995.
- 21 Platt, T., Sathyendranath, S., Forget, M.-H., White III, G. N., Caverhill, C., Bouman, H., Devred,
22 E. and Son, S.: Operational estimation of primary production at large geographical scales.
23 Rem. Sens. Env. 112, 3437-3448, 2008.
- 24 Platt, T., Sathyendranath, S., Joint, I., and Fasham, M. J. R.: Photosynthesis characteristics of
25 phytoplankton in the Celtic Sea during late spring. Fish. Oceanogr. 2, 191-201, 1993.
- 26 Prézelin, B. B., Meeson, B. W., and Sweeney, B. M.: Characterization of photosynthetic rhythms
27 in marine dinoflagellates. 1. Pigmentation, photosynthetic capacity and respiration. Plant
28 Physiol. 60, 384-387, 1977.
- 29 Prézelin, B. B., Putt, M., and Glover, H. E.: Diurnal patterns in photosynthetic capacity and
30 depth-dependent photosynthesis-irradiance relationships in *Synechococcus* spp. and
31 larger phytoplankton in three water masses in the Northwest Atlantic Ocean. Mar. Biol.
32 92: 205-217, 1986.



- 1 Prézelin, B.B., Glover, H. R., Ver Hoven, B. M., Stenberg, D., Matlick, H. A., Schofield, O.,
2 Nelson, N. B., Wyman, M., and Campbell, L.: Blue-green light effects on light-limited
3 rates of photosynthesis: relationship to pigmentation and productivity estimates for
4 *Synechococcus* populations from the Sargasso Sea. *Mar. Ecol. Progr. Ser.* 54, 121-136,
5 1989.
- 6 Puxty, R. J., Millard, A. D., Evans, D. J., and Scanlan, D. J.: Viruses inhibit CO₂ fixation in the
7 most abundant phototrophs on earth. *Curr. Biol.*, 26, 1585–1589, 2016.
- 8 Rey, F.: Photosynthesis-irradiance relationships in natural phytoplankton populations of the
9 Barents Sea. *Polar Res.* 10, 105-116, 1991.
- 10 Sakshaug, E., Bricaud, A., Dandonneau, Y., Falkowski, P. G., Kiefer, D. A., Legendre, L.,
11 Morel, A., Parslow, J., and Takahashi, M.: Parameters of photosynthesis: definitions,
12 theory and interpretation of results. *J. Plankton Res.* 19, 1637–1670, 1997.
- 13 Sathyendranath, S., Stuart, V., Nair, A., Oka, K., Nakane, T., Bouman, H., Forget, M.-H., Maass,
14 H., and Platt, T.: Carbon-to-chlorophyll ratio and growth rate of phytoplankton in the sea.
15 *Mar. Ecol. Progr. Ser.* 383, 73-84, 2009.
- 16 Sathyendranath, S., Stuart, V., Irwin, B.D., Maass, H., Savidge, G., Gilpin, L., and Platt, T.:
17 Seasonal variation in bio-optical properties of phytoplankton in the Arabian Sea (1999)
18 *Deep Sea Res. II*, 46, 633-353, 1999.
- 19 Saux-Picart, S., Sathyendranath, S., Dowell, M., Moore, T., and Platt, T.: Remote sensing of
20 assimilation number for marine phytoplankton. *Remote Sens. Env.* 146, 87-96, 2014.
- 21 Segura, V., Lutz, V. A., Dogliotti, A. I., Silva, R., Negri, R., Akselman, R. and Benavides, H.:
22 Phytoplankton Functional Types and primary production in the Argentine Sea. *Mar. Ecol.*
23 *Prog. Ser.* 491, 15-31, 2013.
- 24 Schofield, O., Prézelin, B. B., Smith, R. C., Stegmann, P. M., Nelson, N. B., Lewis, M. R., and
25 Baker, K. S.: Variability in spectral and nonspectral measurements of photosynthetic light
26 utilization efficiencies. *Mar. Ecol. Prog. Ser.* 78, 253-271, 1991.
- 27 Smith Jr., W.O., Donaldson, K.: Photosynthesis-irradiance responses in the Ross Sea, Antarctica:
28 a meta-analysis. *Biogeosci.* 12, 3567-3577, 2015.
- 29 Smith Jr. W. O., and Donaldson, K.: Photosynthesis-irradiance responses in the Ross Sea,
30 Antarctica: a meta-analysis. *Biogeosci.* doi:10.5194/bg-12-3567-2015, 2015.



- 1 Tilstone, G. H., Figueiras, F. G., Lorenzo, L. M., and Arbones, B.: Phytoplankton composition,
2 photosynthesis and primary production during different hydrographic conditions at the
3 Northwest Iberian upwelling system. *Mar. Ecol. Progr. Ser.* 252, 89-104, 2003.
- 4 Ulloa, O., Hoepffner, N., Larkin, D.: Depth and wavelength dependence of phytoplankton
5 photosynthesis: implications for the remote sensing of marine primary production. *Proc.*
6 *SPIE* 2963, *Ocean Optics XIII*; doi: 10.1117/12.266456, 1997.
- 7 Westwood K. J., Griffiths F. B., Webb J. P., Wright S. W.: Primary production in the Sub-
8 Antarctic and Polar Frontal zones south of Tasmania, Australia; SAZ-Sense survey, 2007.
9 *Deep Sea Res. Part II* 58, 2162–2178, 2011.
- 10 Xie, Y., Bangqin, H., Lin, L., Laws, E. A., Wang, L., Shang, S., Zhang, T., and Dai, M.:
11 Photosynthetic parameters in the northern South China Sea in relation to phytoplankton
12 community structure. *J. Geophys. Res.* DOI 10.1002/2014JC010415, 2015.
- 13 Zhai, L., Gudmundsson, K., Miller, P., Peng, W., Guðfinnsson, H., Debes, H., Hátún, H., White
14 III, G.N., Walls, R.H., Sathyendranath, S., and Platt, T.: Phytoplankton phenology and
15 production around Iceland and Faroes. *Cont. Shelf Res.* 37, 15-25, 2012.
- 16 Zwirgmaier, K., Heywood, J. L., Chamberlain, K., Woodward, E. M. S., Zubkov, M. V.,
17 Scanlan, D. J. 2007. Basin-scale distribution patterns of picocyanobacterial lineages in
18 the Atlantic Ocean. *Environ. Microbiol.* 9, 1278-1290, 2007.
- 19
- 20
- 21



Table 1: Numbers corresponding to Biogeochemical Province and Domain as described by Longhurst 2007 included in the MAPPS database.

Province Number	Longhurst Domain	Longhurst Province
1	Polar	Boreal Polar Province
2	Polar	Atlantic Arctic Province
3	Polar	Atlantic Subarctic Province
4	Westerlies	North Atlantic Drift Province
5	Westerlies	Gulf Stream Province
6	Westerlies	North Atlantic Subtropical Gyre Province (West)
7	Trades	North Atlantic Tropical Gyre Province
8	Trades	Western Tropical Atlantic Province
9	Trades	Eastern Tropical Atlantic Province
10	Trades	South Atlantic Gyre Province
11	Coastal	North East Atlantic Shelves Province
12	Coastal	Canary Coastal Province
15	Coastal	North West Atlantic Shelves Province
17	Trades	Caribbean Province
18	Westerlies	North Atlantic Subtropical Gyre Province (East)
20	Coastal	Brazil Current Coastal Province
21	Coastal	South West Atlantic Shelves Province
22	Coastal	Benguela Current Coastal Province
30	Trades	Indian Monsoon Gyres Province
33	Coastal	Red Sea, Persian Gulf Province
34	Coastal	North West Arabian Upwelling Province
37	Coastal	Australia-Indonesia Coastal Province
50	Polar	North Pacific Epicontinental Province
51	Westerlies	Pacific Subarctic Gyres Province (East)
53	Westerlies	Kuroshio Current Province
58	Westerlies	Tasman Sea Province
60	Trades	N. Pacific Tropical Gyre Province
63	Trades	W. Pacific Warm Pool Province
64	Trades	Archipelagic Deep Basins Province
68	Coastal	Chile-Peru Current Coastal Province
69	Coastal	China Sea Coastal Province
80	Westerlies	S. Subtropical Convergence Province
81	Westerlies	Subantarctic Province
82	Polar	Antarctic Province
83	Polar	Austral Polar Province

**Table 2: Summary of contributions to the MAPPS database.**

Dataset Provider	Regions	Dates	<i>N</i>	Non-linear equation(s) fitted to experimental data	Database	Relevant Publication(s)
Prof. Trevor Platt Plymouth Marine Laboratory (tplatt@dal.ca)	Arctic, Arabian Sea, Azores, Caribbean Sea, Celtic Sea, Georges Bank, Grand Banks, Humboldt Current System, Hudson Bay, Labrador Sea, Mid- Atlantic Ridge, New England Seamounts Sargasso Sea, Scotian Shelf, Vancouver Island	1977- 2003	2146	Photoinhibition function (Platt et al. 1980)	BIOCHEM (www.meds-sdmm.dfo-mpo.gc.ca)	Bouman et al. (2005) Deep- Sea Res Pt I; Harrison and Platt (1986) Polar Biol; Kyewalyanga et al. (1998) J Plankton Res; Platt et al. (1980) J Mar Res; Platt et al. (1982) Deep-Sea Res Pt I; Platt et al. (1993) Fish Oceanogr; Sathyendranath et al (1999)
Dr. Francisco Rey Institute of Marine Research (pancho@IMR.no)	Barents Sea	1980- 1989	223	Photoinhibition function (Platt et al. 1980)		Rey (1991) Polar Res
Dr. Pierre Pepin Fisheries and Oceans Canada, Northwest Atlantic Fisheries Centre (pierre.pepin@dfo-mpo.gc.ca)	Grand Banks	2004- 2012	524	Photoinhibition function (Platt et al. 1980)		Unpublished
Dr. Heather Bouman University of Oxford (Heather.Bouman@earth.ox.ac.uk)	Subtropical Atlantic, Greenland Sea, Norwegian Sea	1996, 2010, 2013	195	Photoinhibition function (Platt et al. 1980)		Bouman et al. (2000) Mar Ecol Prog Ser; Jackson (2013) DPhil Thesis, U Oxford, Bouman (unpublished)
Dr. Michael Hiscock National Center for Environmental Research US Environmental Protection Agency (Hiscock.Michael@epa.gov)	Southern Ocean – Pacific Sector	1997- 1998	172	Photoinhibition function (Platt et al. 1980)		Hiscock (2004) PhD Thesis – Duke U; Hiscock et al. (2003) Deep- Sea Res Pt II
Dr. Vivian Lutz Instituto Nacional de Investigación y Desarrollo Pesquero (vlutz@inidep.edu.ar)	Argentine Sea	2005- 2006	69	Photoinhibition function (Platt et al. 1980)		Dogliotti et al. (2014) Remote Sens Environ; Lutz et al. (2010) J Plankton Res; Segura et al. (2013) Mar Ecol Prog Ser
Dr. Gavin Tilstone Plymouth Marine Laboratory (ghti@pml.ac.uk)	Benguela upwelling system, Eastern Tropical Atlantic, North Atlantic Subtropical Gyre, Canary coastal system, North Atlantic Drift province	1998	129	Photoinhibition function (Platt et al. 1980)	BODC (www.bodc.ac.uk)	Tilstone et al. (2003) Mar Ecol Prog Ser



Dr. Bangqin Huang State Key Laboratory of Marine Environmental Sci- ence/Key Laboratory of Coastal and Wetland Ecosystems Ministry of Education, Xiamen University (bqhuang@xmu.edu.cn)	South China Sea	2010- 2012	130	Photoinhibition function (Platt et al. 1980)		Xie et al. (2015) J. Geophys. Res.
Dr. Anna Hickman National Oceanography Centre Southampton (A.Hickman@noc.soton.a c.uk)	North Atlantic Subtropical Gyre, North Atlantic Drift province, Canary coastal system, South Atlantic Subtropical Gyre, Western Tropical Atlantic	2004	31	Hyperbolic tangent function (Jassby and Platt 1976).	BODC (www.bodc.ac.uk)	Hickman (2007) PhD Thesis – U Southampton; Lawrenz et al. 2013 PLOS-ONE
Dr. Kristinn Gudmundsson Marine Research Institute, Iceland (kristinn@hafro.is)	Iceland and Faroes	1981- 2007	559	Photoinhibition function (Platt et al. 1980) and hyperbolic tangent function (Jassby and Platt 1976).		Gudmundsson (1998) ICES J Mar Sci; Pálsson et al. (2012) ICES J Mar Sci; Zhai et al. (2012) Cont Shelf Res
Prof. Francisco G. Figueiras, Instituto de Investigaciones Marinas (CSIC) Eduardo Cabello 6, 36208 Vigo, Spain (paco@iim.csic.es)	Antarctic Peninsula	1995	51	Exponential without photoinhibition Webb et al. (1975)	JGOFS International Collection Volume 1: Discrete Datasets (1989- 2000) DVD	Lorenzo, L.M. et al. (2002) Deep Sea Res II
Dr. Martina Doblin University of Technology, Sydney (Martina.Doblin@uts.edu. au)	Southern Ocean, Antarctic Peninsula, Tasman Sea	1990- 2013	1482	Photoinhibition function (Platt et al. 1980)	AADC (https://data.aad.gov.au/aadc/metadata/) MARLIN (http://www.marine.csiro.au/marq/edd_search.search_choice?tfre=primary+production&chl=freetext&cSub=%3E%3E) CSIRO Marine National Facility (http://www.marine.csiro.au/nationalfacility/voyages/datasets.htm) PANGAEA (http://doi.pangaea.de/10.1594/PANGAEA.103773 , http://doi.pangaea.de/10.1594/PANGAEA.843554 ,	Mackey et al. (1995) DSR II; Griffiths et al. (1999) J Geophys Res; Hanson et al. (2005) Cont Shelf Res; Hanson et al. (2005) Mar Freshwater Res; Westwood et al. (2011) Deep-Sea Res Pt II



Table 3: List of environmental variables and P-E parameters in the MAPPS database and their corresponding units.

Header	Description	Units
LAT	Latitude of sampling station.	Decimal degrees
LON	Longitude of sampling station.	Decimal Degrees
DEPTH	Depth at which sample was collected.	m
YEAR	Year of sample collection.	
MONTH	Month of sample collection.	
DAY	Day of sample collection	
TCHL	Chlorophyll concentration measured using either High Performance Liquid Chromatography or the fluorometric method.	mg chl-a m ⁻³
ALPHA	α^B , the initial slope of the photosynthesis-irradiance curve normalised to phytoplankton chlorophyll concentration.	mg C (mg chl-a) ⁻¹ h ⁻¹ ($\mu\text{mol quanta m}^{-2} \text{s}^{-1}$) ⁻¹
PMB	P_m^B , the rate of photosynthesis at saturating irradiance, normalised to phytoplankton chlorophyll concentration.	mg C (mg chl-a) ⁻¹ h ⁻¹
EK	E_k , irradiance at which the onset of saturation occurs, calculated as the ratio of P_m^B to α^B .	$\mu\text{mol quanta m}^{-2} \text{s}^{-1}$
PROVNUM	The corresponding biogeochemical province defined by Longhurst (please refer to Table 2).	

5

10

15

20



Table 4. Information on the light sources and filters used for photosynthesis-irradiance experiments for each of the dataset providers. Also noted is whether the spectral correction of Kyewalyanga et al. (1997) shown in equation was applied to values of α^B .

Dataset provider	Lamp Source Details	Spectral Correction
Platt	GTE Sylvania PAR 150	N
	Combination of GTE Sylvania PAR 150 (irradiances < 200 W) and New Haline OHS tungsten halogen (irradiances 200-1000 W)	N
	2000 W tungsten-halogen lamp (New Haline OHS 2000) with a maximum intensity of 1000 W m ⁻² (PAR)	N
	Gilway Technical Lamp L 7391 tungsten halogen. Spectral correction applied to samples collected from 1994 onwards.	Y
Rey	Low-light incubator (LL, 0 to 390 mmol m ⁻² s ⁻¹) was equipped with daylight-type fluorescent tubes (OSRAM 191 Daylight 5000 de Luxe). High-light incubator (HL, 0 to 1700 μmol m ⁻² s ⁻¹), was equipped with a halogen-metal lamp (OSRAM Power Star, 400 W).	N
Pepin	ENH-type tungsten-halogen quartz projection lamps directed through a heat filter (solution of copper sulfate 20g L ⁻¹) to remove the infrared emission (no additional corrections made).	N
Bouman	Gilway Technical Lamp L 7391 tungsten halogen, Spectral correction applied.	Y
	Lee ¼ CT blue filter was placed in front of incubator window to diminish the spectral dependency of the light source (2 x 50 W Sylvania 2315 tungsten halogen). Spectral correction applied.	Y
Hiscock	250 W tungsten-halogen slide projector lamp (Gray Co. #ENH), spectrally modified using a heat mirror, a broad band cool mirror (Optical Coating Laboratory, Inc.), and blue stage-lighting screens (Cinemills Corp. #M144).	Y
Lutz	70 W Westinghouse halogen lamp. Spectral correction applied.	Y
Tilstone	AMT 6 and 20: tungsten-halogen lamps spectrally corrected. AMT 23: both tungsten-halogen and LED lamps used and spectrally corrected.	Y
Huang	150 W metal halide lamps with an ultraviolet filter. Spectral correction applied.	Y
Hickman	Tungsten halogen lamps behind blue light filters (no additional corrections made).	N
Figueiras	50W (12V) tungsten halogen lamp. Spectral correction applied.	Y
Gudmundsson	Fluorescent tubes (Philips TLF 20W/33). No additional corrections made.	N
Doblin	Cool Daylight fluorescent tubes (Philips TLD 36W/54). A mix of grey and blue filters (Rosco 3402, 50% neutral density filter, i.e. grey strips, and Rosco 3204 half blue) were used to attenuate the light intensity in the incubator.	N



Table 5: Seasonal mean values and standard deviation for the photosynthetic parameters P_m^B and α^B for each of the 35 Longhurst Provinces. The blocked colours represent the four primary biomes of the upper ocean: Polar (blue), Westerlies (yellow), Trades (orange) and Coastal (green).

PROV	Spring					Summer					Autumn					Winter				
	P_m^B	α^B				P_m^B	α^B				P_m^B	α^B				P_m^B	α^B			
	N	Mean	Stdev	Mean	Stdev	N	Mean	Stdev	Mean	Stdev	N	Mean	Stdev	Mean	Stdev	N	Mean	Stdev	Mean	Stdev
BPLR	194	1.86	0.91	0.037	0.032	385	1.93	1.29	0.030	0.031	50	2.10	1.12	0.029	0.022	13	1.56	0.76	0.019	0.007
ARCT	421	2.46	1.52	0.047	0.031	203	2.38	1.27	0.042	0.028	37	2.53	0.84	0.056	0.032	18	2.30	0.73	0.023	0.008
SARC	150	2.67	1.18	0.046	0.023	41	3.08	2.38	0.045	0.022	2	1.40	0.46	0.088	0.045	0				
ANTA	79	3.55	1.69	0.101	0.047	145	3.50	1.70	0.051	0.023	78	3.50	1.70	0.051	0.023	22	4.18	2.21	0.096	0.026
APLR	119	1.84	1.22	0.044	0.023	222	1.79	1.05	0.042	0.019	12	1.79	1.05	0.042	0.019	0				
BERS	3	3.43	2.03	0.059	0.043	0					0					0				
NADR	40	3.49	1.13	0.033	0.010	5	4.41	4.64	0.029	0.025	48	2.10	1.06	0.028	0.018	0				
GFST	55	4.41	2.40	0.031	0.013	12	3.57	2.30	0.016	0.007	32	3.41	1.85	0.056	0.039	0				
NASW	85	5.92	3.30	0.026	0.014	91	1.72	1.34	0.025	0.022	35	3.67	2.15	0.066	0.072	0				
NASE	15	2.63	1.42	0.030	0.006	6	4.02	1.88	0.031	0.013	37	3.17	2.65	0.057	0.042	0				
PSAE	0					0					2	3.41	1.05	0.034	0.010	0				
TASM	0					7	2.89	1.59	0.057	0.022	16	7.18	2.20	0.070	0.017	0				
SSTC	50	6.81	4.58	0.076	0.033	116	3.10	2.19	0.035	0.025	6	4.24	0.37	0.035	0.008	6	6.36	2.94	0.066	0.008
SANT	162	4.67	2.35	0.085	0.040	165	3.34	2.19	0.066	0.041	107	3.88	1.55	0.054	0.018	14	4.69	1.94	0.075	0.024
KURO	6	9.25	4.25	0.027	0.009	0					1	10.50		0.023		0				
NATR	6	3.33	2.29	0.037	0.017	66	2.54	1.50	0.057	0.048	20	2.97	2.69	0.041	0.035	0				
WTRA	17	1.34	0.63	0.022	0.020	0					0					8	5.08	4.53	0.064	0.015
ETRA	0					0					11	3.00	0.96	0.027	0.011	0				
SATL	48	1.29	0.65	0.027	0.024	0					2	3.58	2.47	0.028	0.016	0				
CARB	20	3.71	2.16	0.011	0.005	0					15	2.15	1.75	0.026	0.020	0				
MONS	0					0					62	4.05	2.04	0.024	0.007	4	5.66	1.60	0.026	0.005
WARM	0					64	2.23	1.67	0.039	0.027	167	2.44	1.65	0.032	0.019	18	3.89	3.09	0.034	0.030
ARCH	70	3.62	3.41	0.034	0.016	0					30	5.86	3.72	0.025	0.009	0				
NPTG	0					0					4	2.62	1.99	0.054	0.074	0				
CHIL	7	2.50	0.93	0.029	0.004	0					0					0				
NECS	29	3.20	1.07	0.023	0.010	0					1	2.22		0.062		0				
CNRY	0					0					23	4.62	1.40	0.065	0.017	0				
AUSW	44	3.04	2.02	0.038	0.015	15	2.61	1.93	0.042	0.026	16	2.12	1.67	0.032	0.017	0				
BRAZ	9	2.37	1.86	0.041	0.035	5	3.63	2.05	0.014	0.005	0					1	0.87		0.019	
REDS	0					4	4.13	2.07	0.022	0.006	0					0				
ARAB	0					132	4.07	1.67	0.021	0.008	79	5.61	1.85	0.027	0.007	0				
FKLD	25	2.96	2.85	0.040	0.035	1	1.71		0.010		19	1.85	1.00	0.017	0.006	9	1.06	0.43	0.012	0.003
BENG	0					0					20	3.82	2.13	0.027	0.011	0				
CHIN	24	7.50	3.68	0.029	0.012	37	6.87	5.18	0.023	0.016	17	8.92	4.45	0.033	0.015	0				
NWCS	306	2.20	1.28	0.024	0.015	219	3.16	1.88	0.016	0.012	188	4.59	1.82	0.044	0.019	9	2.91	1.62	0.039	0.019

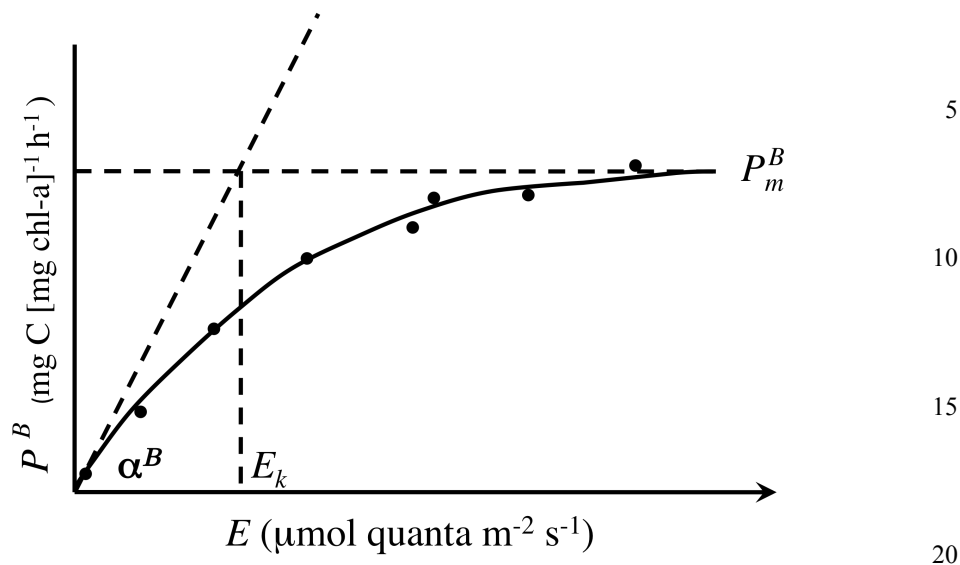


Figure 1: Photosynthesis-irradiance (P-E) curve showing the two biomass-normalised photophysiological parameters, the maximum photosynthetic rate P_m^B and the initial slope α^B .

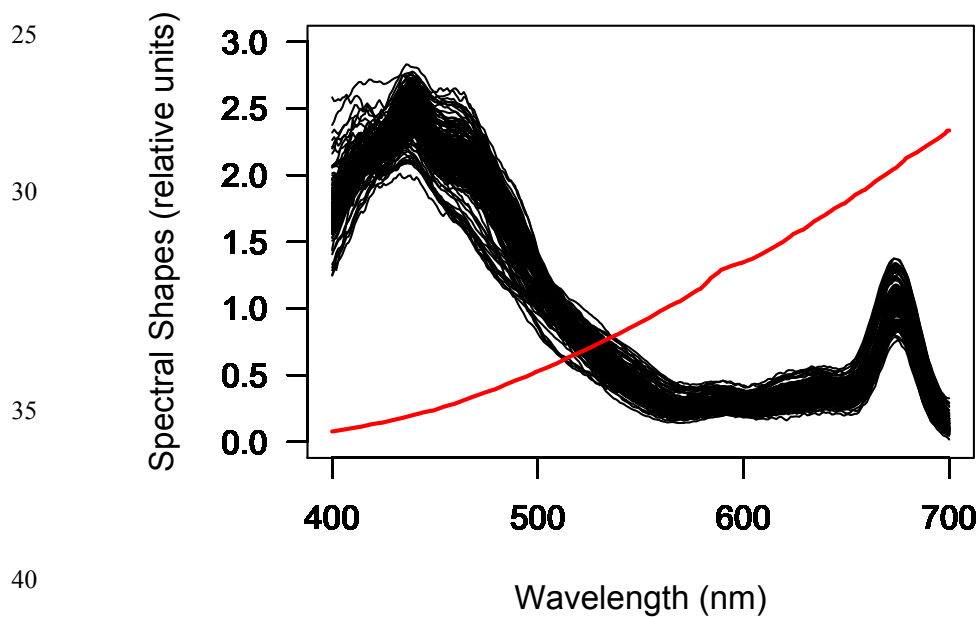


Figure 2: Spectral shapes of the tungsten-halogen lamp used in the incubations conducted by the Bedford Institute from 1984 to 2003 (red line) and *in vivo* absorption spectra of marine phytoplankton collected in the North Atlantic and subpolar waters (Labrador Sea). Phytoplankton and lamp spectra were normalised to their mean value to define the shape

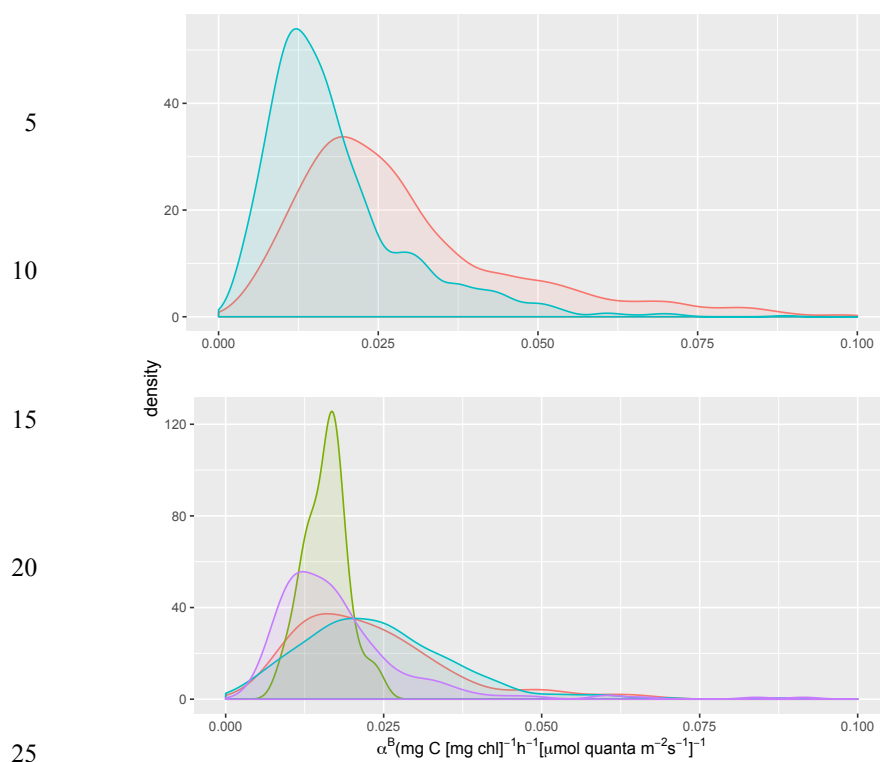


Fig. 3 a) Density plots of the initial slope (α^B) obtained using a tungsten halogen lamp (cyan) and corrected values using the shape of the phytoplankton absorption spectrum (red) as described in Kyewalyanga et al. 1997. b) Density plots of data collected in the North Atlantic using different lamp types (red - GTE Sylvania PAR 150; green – Combination of GTE Sylvania PAR 150 (irradiance < 200 W) and New Haline OHS tungsten halogen (irradiance 200-1000 W); cyan – New Haline OHS 2000 tungsten halogen; purple – Gilway Technical Lamp L 7391 tungsten halogen). Both plots are using data collected within the top 20 m of the watercolumn.

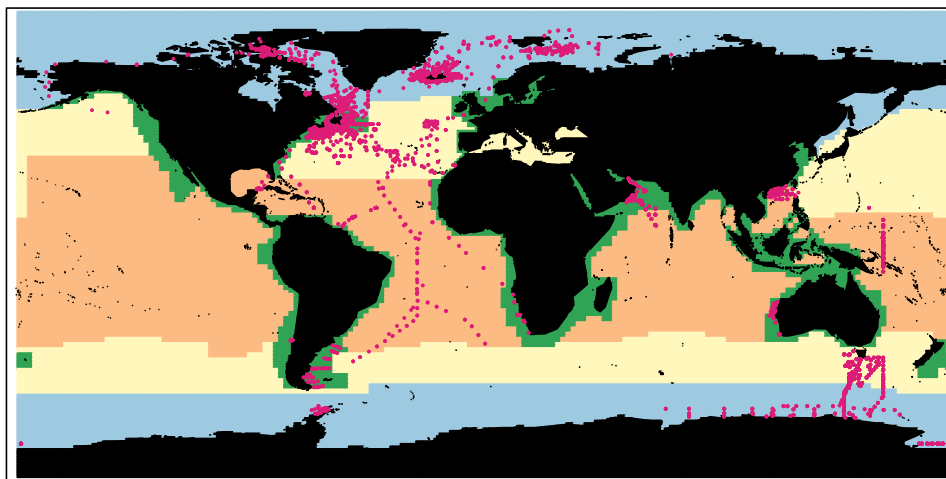


Figure 4: Global distribution of MAPPS *P-E* dataset that passed quality control (5711 samples).

The blocked colours represent the four primary biomes as described in Longhurst (2007): Polar
5 **(blue), Westerlies (yellow), Trades (orange) and Coastal (green).**

10

15

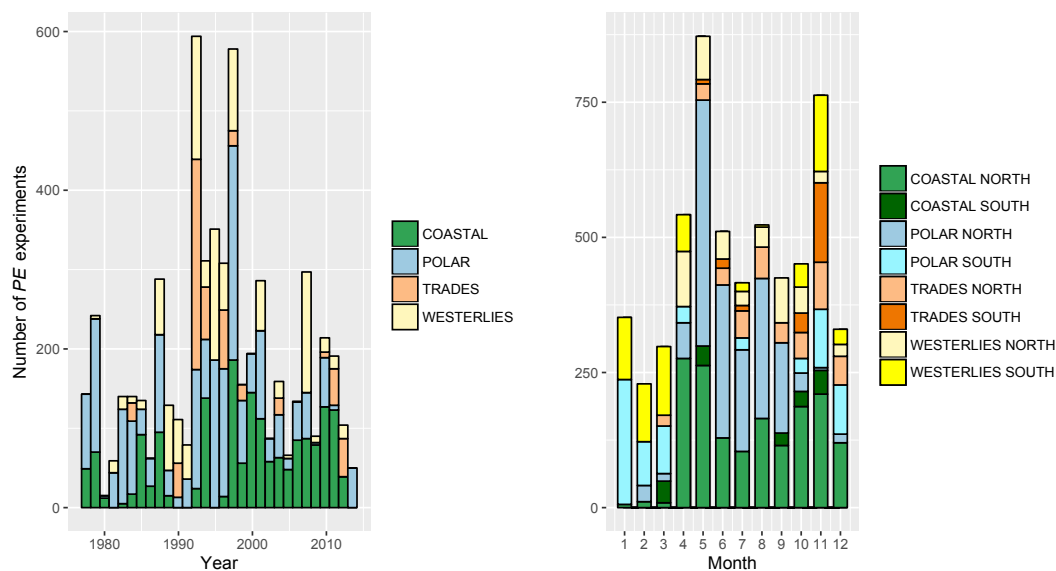


Figure 5: The number of PE experiments in the MAPPS database for the four Longhurst oceanic domains by a) year and b) month and hemisphere (North and South).

5

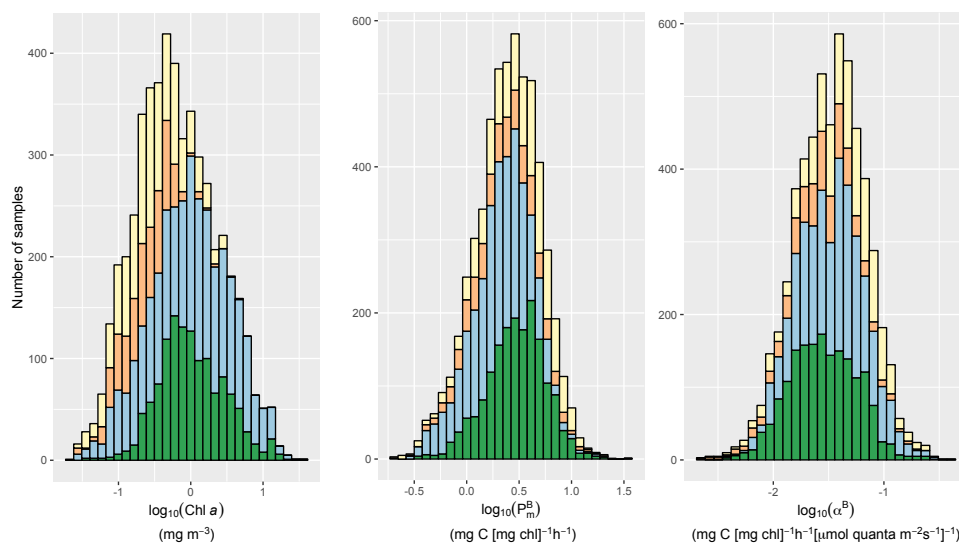


Figure 6: Histograms illustrating the sample distribution across concentrations of chlorophyll-a and range of PE parameter values for the four Longhurst oceanic domains.

10

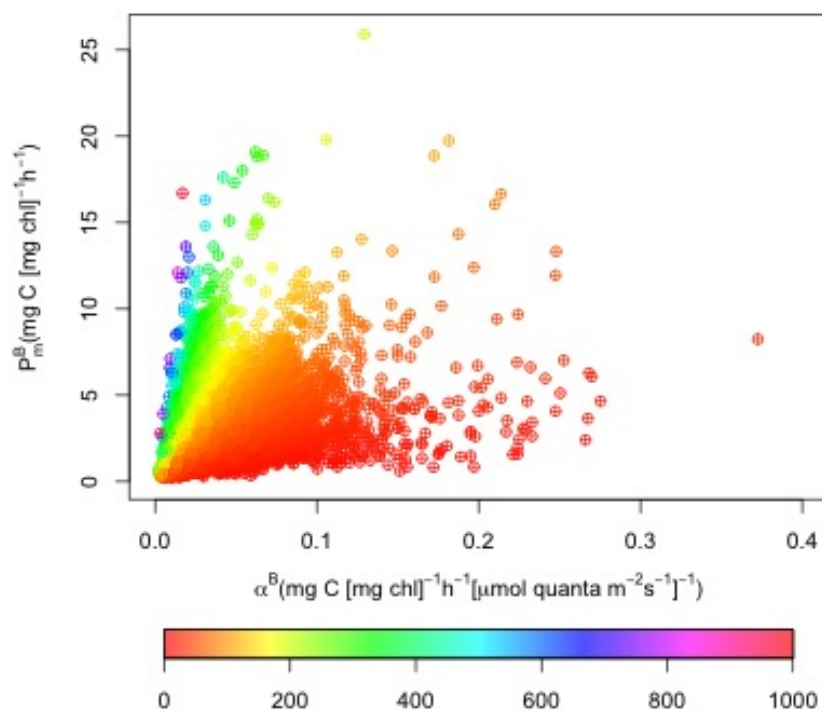


Figure 7: The assimilation number (P_m^B) plotted against the initial slope (α^B). Symbol colours represent the value of E_k in units of $\mu\text{mol quanta m}^{-2} \text{s}^{-1}$.

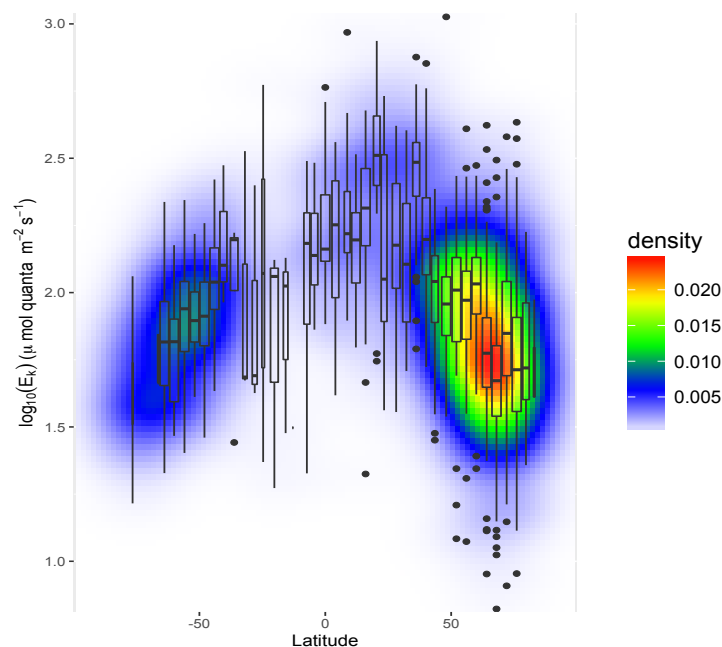


Figure 8: Density plot and box plots showing the variation in the photoadaptation parameter (E_k) with latitude. Middle horizontal line of boxplot represents the median value and lower and upper hinges correspond to the first and third quartiles and the length of the whiskers 1.5 times the inter-quantile range of the hinge. Filled circles denote outliers.

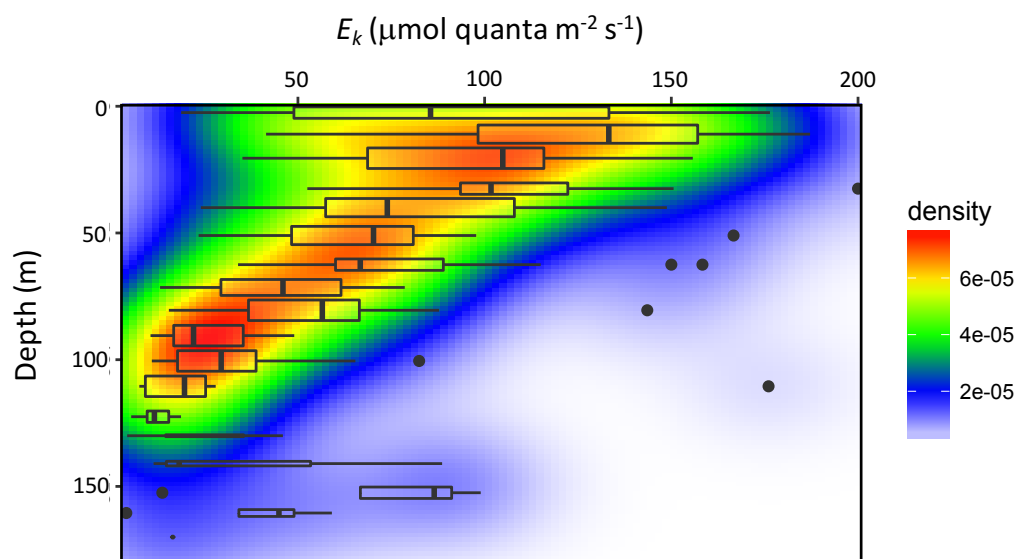


Figure 9: Density plot and box plots showing variation in the photoadaptation parameter (E_k) with depth for research cruises focussed on the oligotrophic gyres (DCM, AMT6, AMT15, AMT20 and AMT22). Middle horizontal line of boxplot represents the median value and lower and upper hinges correspond to the first and third quartiles and the length of the whiskers 1.5 times the inter-quantile range of the hinge. Filled circles denote outliers.